2-2-2009

Acceptance angle effects on the beam attenuation in the ocean

Emmanuel Boss
University of Maine, emmanuel.boss@maine.edu

Wayne H. Slade
University of Maine

M. Behrenfeld
Oregon State University, emmanuel.boss@maine.edu

G. Dall'Olmo
Oregon State University

Acceptance angle effects on the beam attenuation in the ocean

Emmanuel Boss[1]*, Wayne H. Slade[2], M. Behrenfeld[3] and G. Dall'Olmo[3]

[1]*School of Marine Sciences, 458 Aubert Hall, University of Maine, Orono, Maine 04401, USA*
[2]*School of Marine Sciences, 461B Aubert Hall, University of Maine, Orono, Maine 04401, USA*
[3]*Department of Botany and Plant Pathology, 2082 Cordley Hall, Oregon State University, Corvallis, OR 97331-2902, USA*
** Corresponding author: emmanuel.boss@maine.edu*

Abstract: The beam attenuation serves as a proxy for particulate matter and is a key parameter in visibility algorithms for the aquatic environment. It is well known, however, that the beam attenuation is a function of the acceptance angle of the transmissometer used to measure it. Here we compare eight different transmissometers with four different acceptance angles using four different deployment strategies and sites, and find that their mean attenuation values differ markedly and in a consistent way with instrument acceptance angle: smaller acceptance angles provide higher beam attenuation values. This difference is due to variations in scattered light collected with different acceptance angles and is neither constant nor easy to parameterize. Variability (in space or time) in the ratios of beam attenuations measured by two different instruments correlates, in most cases, with the particle size parameter (as expected from Mie theory), but this correlation is often weak and can be the opposite of expectations based on particle size changes. We recommended careful consideration of acceptance angle in applications of beam transmission data especially when comparing data from different instruments.

OCIS codes: (010.0010) Atmospheric and oceanic optics; (010.4458) Oceanic scattering (120.5820) Scattering measurements; (290.2200) Extinction; (290.2558) Forward scattering; (290.5850) Scattering, particles.

References and links

1. N. G. Jerlov, "Marine optics," in *Suspended Solids in Water*, R. J. Gibbs, ed. (Plenum Press, Elsevier, Amsterdam, 1976).
2. R. W. Spinrad, J. R. V. Zaneveld, and J. C. Kitchen, "A study of the optical characteristics of the suspended particles in the benthic nepheloid layer of the Scotian shelf," J. Geophys. Res. **88**, 7641–7645 (1983).
3. R. J. Gibbs, *Suspended Solids in Water* (Plenum Press, 1974).
4. E. T. Baker and J. W. Lavelle, "The effect of particle size on the light attenuation coefficient of natural suspensions," J. Geophys Res. **89**, 8197–8203 (1984).
5. W. D. Gardner, I. D. Walsh, and M. J. Richardson , "Biophysical forcing of particle production and distribution during a spring bloom in the North Atlantic," Deep-Sea Res. II, **40**, 171-195 (1993).
6. J. K. B. Bishop, "Transmissometer measurement of POC," Deep-Sea Res. I **46**, 353-369 (1999).
7. H. C. van de Hulst, *Light Scattering by Small Particles* (Dover, 1981).
8. K. J. Voss and R. W. Austin, "Beam-attenuation measurements error due to small-angle scattering acceptance," J. Atmos. Oceanic Technol. **10**, 113–121 (1993).
9. W. S. Pegau, J. R. V. Zaneveld, and K. J. Voss, "Toward closure of the inherent optical properties of natural waters," J. Geophys. Res. **100**, 193 – 199 (1995).
10. X. Quan and E. S. Fry, "An empirical expression for the index of refraction of seawater," Appl. Opt. **34,** 3477–3480 (1995).
11. T. J. Petzold, "Volume scattering functions for selected ocean waters," Tech. Rep. SIO **72-78**, Scripps Institution of Oceanography, San Diego, Calif. (1972).
12. M. Jonasz and E. Boss, "Volume scattering function at the small angles," Top. Part. Disp. Sci. (2006), www.tpdsci.com/Tpc/VsfSmlAngNatDsp.php.

#104741 - $15.00 USD Received 4 Dec 2008; revised 15 Jan 2009; accepted 16 Jan 2009; published 26 Jan 2009

13. D. J. Bogucki, J. A. Domaradzki, D. Stramski, and R. Zaneveld, "Near-forward scattering on turbulence - comparison with scattering on oceanic particulates," Appl. Opt. **37**, 4669–4677 (1998).
14. D. J. Bogucki, J. A. Domaradzki, R. E. Ecke, and C. R. Truman, "Light scattering on oceanic turbulence," Appl. Opt. **43**, 5662-5668 (2004).
15. O. A. Mikkelsen, T. G. Milligan, P. S. Hill, R. J. Chant, C. F. Jago1, S. E. Jones, V. Krivtsov, and G. Mitchelson-Jacob, "The influence of schlieren on in situ optical measurements used for particle characterization," Limnol. Oceanogr. Methods **6**, 133–143 (2008).
16. J. K. B. Bishop and T. J. Wood, "Particulate matter chemistry and dynamics in the twilight zone at VERTIGO ALOHA and K2 sites," Deep-Sea Res. I **55**, 1684-1706 (2008).
17. M. Jonasz and G. Fournier, *Light Scattering by Particles in Water: Theoretical and Experimental Foundations* (Academic Press, 2007).
18. J. R. Zaneveld and W. S. Pegau, "Robust underwater visibility parameter," Opt. Express **11**, 2997-3009 (2003).
19. M. J. Behrenfeld and E. Boss, "Beam attenuation and chlorophyll concentration as alternative optical indices of phytoplankton biomass," J. Mar. Res. **64**, 431–451 (2006).
20. H. Loisel, X. Mériaux, J. F. Berthon, and A. Poteau, "Investigation of the optical backscattering to scattering ratio of marine particles in relation to their biogeochemical composition in the eastern English Channel and southern North Sea," Limnol. Oceanogr. **52**, 739-752 (2007).
21. W. H. Slade and E. Boss, "Calibrated Near-Forward Volume Scattering Function Obtained from the LISST Particle Sizer," Opt. Express **14**, 3602-3615 (2006).
22. G. Dall'Olmo, T. K. Westberry, M. J. Behrenfeld, E. Boss, and W. H. Slade, "Direct contribution of phytoplankton-sized particles to optical backscattering in the open ocean" submitted to Biogeosciences.
23. W. H. Slade and E. Boss, "Significant of particle aggregation on optical properties", Proceedings of the Ocean Optics XIX conference (2008).
24. M. S. Twardowski, J. M. Sullivan, P. L. Donaghay, and J. R. V. Zaneveld, "Microscale quantification of the absorption by dissolved and particulate material in coastal waters with an ac-9," J. Atmos. Ocean. Technol. **16**, 691–707 (1999).
25. E. Boss, W. S. Pegau, W. D. Gardner, J. R. V. Zaneveld, A. H. Barnard, M. S. Twardowski, G. C. Chang, and T. D. Dickey, "Spectral particulate attenuation and particle size distribution in the bottom boundary layer of a continental shelf," J. Geophys. Res. **106**, 9509-9516 (2001).
26. A. A. Kokhanovsky, *Light scattering media optics* (Springer, Praxis, 2004).
27. Y. C. Agrawal and H. C. Pottsmith, "Instruments for particle size and settling velocity observations in sediment transport," Marine Geology **168**, 89-114 (2000).
28. D. A. Siegel, "Resource competition in a discrete environment: Why are plankton distributions paradoxical?," Limnol. Oceanogr. **43**, 1133-1146 (1998).
29. H. Pak, D. A. Kiefer, and J. C. Kitchen "Meridional variations in the concentration of chlorophyll and microparticles in the North Pacific Ocean," Deep-Sea Res. **35**, 1151-1171 (1988).
30. J. Trowbridge, Woods Hole Oceanographic Institution, Bigelow 105A, MS#12, Woods Hole, Ma. 02543 (personal communication, 2005).
31. D. A. Siegel, "Optical determination of particulate abundance and production variations in the oligotrophic ocean," Deep-Sea Res. Part A **36**, 211-222 (1989).
32. M. Stramska and T. D. Dickey, "Variability of bio-optical properties of the upper ocean associated with diel cycles in phytoplankton population," J. Geophys. Res. **97**, 17873-17887 (1992).
33. M. D. DuRand, and R. J. Olson, "Contributions of phytoplankton light scattering and cell concentration changes to diel variations in beam attenuation in the equatorial Pacific from flow cytometric measurements of pico-, ultra-, and nanoplankton," Deep-Sea Research II, **43**, 891-906 (1996).
34. I. D. Walsh, S. P. Chung, M. J. Richardson, and W. D. Gardner, "The Diel Cycle in the Integrated Particle Load in the Equatorial Pacific: A Comparison with Primary Production," Deep-Sea Res. II, **42**, 465–478 (1995).
35. H. Claustre, Y. Huot, I. Obernosterer, B. Gentili, D. Tailliez, and M. Lewis, "Gross community production and metabolic balance in the South Pacific Gyre, using a non intrusive bio-optical method," Biogeosciences **5**, 463-474 (2008).

1. Introduction

For nearly six decades, beam attenuation has been measured in water [1]. It has been used to estimate the concentration of suspended particles in aquatic environments by correlating it with particle volume [2], total mass (e.g. see [3,4]), and particulate organic carbon (POC, e.g. see [5,6]).

The beam attenuation (c, [m^{-1}]) of a suspension is calculated from light transmission (T), defined as the ratio of intensity of light reaching a receiver through a sample ($I_{suspension}$ [W]),

#104741 - $15.00 USD Received 4 Dec 2008; revised 15 Jan 2009; accepted 16 Jan 2009; published 26 Jan 2009

relative to the light intensity reaching the receiver through a blank material (I_{blank}, [W], most often the purest water available), $T \equiv I_{suspension} / I_{blank}$,. Together with the instrument pathlength (L, [m]), the beam attenuation is (e.g. see [7]):

$$c = -\frac{1}{L} ln(T). \quad (1)$$

The beam attenuation is unique among the inherent optical properties in that it does not have to be corrected using other measurements (no scattering or attenuation along-the-path correction needs to be applied). It is, however, assumed that measurements are made in the single-scattering regime (i.e. the probability for a multiple scattering event is negligible when compared to that for a single scattering event). In most modern instruments, the intensity of the light source during a measurement is tracked independently (e.g. using a beam-splitter) and Eq. (1) is modified to include changes in source intensity. When water is used as a reference material, the value of the water attenuation needs to be added to that computed from Eq. (1) to obtain the total attenuation coefficient. If air is used as the reference for measurement of an aquatic suspension, the difference in reflection coefficient between air and water at the windows needs to be accounted for before the blank reading can be used.

Beam attenuation is the sum of absorption (a, [m^{-1}]) and scattering (b, [m^{-1}]). Scattering is the integral over all directions of the volume scattering function (β, [m^{-1} sr^{-1}]), which is assumed to be azimuthally symmetric (e.g. due to random particle orientation), and thus:

$$b_{theory} = 2\pi \int_0^{\pi} \beta \sin\theta d\theta. \quad (2)$$

In the most commonly-available commercial transmissometers [8] the light emanating from a source is first collimated by a lens, then passed through a window into a sample of interest, and then, following a passage through another window, focused by a lens onto a detector.

Given the need for a detector with a finite area in order to obtain a signal, the acceptance angle, $\theta_{acceptance}$, of the instrument is also finite and some forward scattered light is always collected by the detector [8,9]. Thus, in practice:

$$c_{measured} = a + 2\pi \int_{\theta_{acceptance}}^{\pi} \beta \sin\theta d\theta. \quad (3)$$

The acceptance angle is calculated from the radius of the aperture (r), the focal distance of the lens (f) and the ratio between the index of refraction of the fluid in which scattering occurs relative to the air within the instrument (n, Snell's law):

$$\theta_{acceptance} = \sin^{-1}\left\{\frac{1}{n}\sin\left[\tan^{-1}\left(\frac{r}{f}\right)\right]\right\}. \quad (4)$$

Note that Jerlov did not include Snell's law in his formulation of the acceptance angle [1]. For measurements in seawater at 660nm, the index of refraction is approximately: n=1.34 [10].

Using Petzold's historical observations [11], Jerlov estimated the bias in the beam attenuation to be about 7% if the acceptance angle is 1° [1]. Revisiting the same data, Jonasz and Boss estimated that about 36% of scattering was from 0-1° [12]. Here we show that this fraction is not constant in many environments and varies on short time scales.

#104741 - $15.00 USD Received 4 Dec 2008; revised 15 Jan 2009; accepted 16 Jan 2009; published 26 Jan 2009

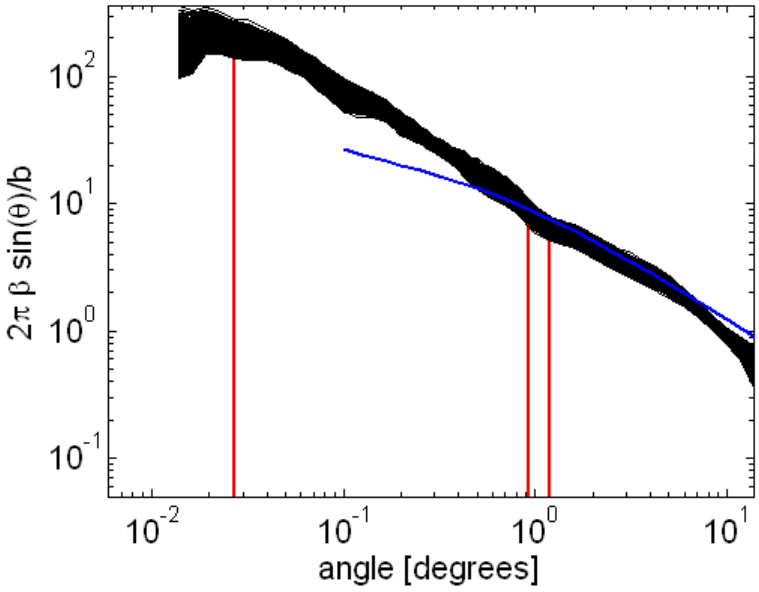

Fig. 1. Normalized volume scattering function as function of angles from Petzold's average phase function ([11], blue curve) and measurements from MVCO (for 9/5/2005, see methods) [11]. The area under the curves to the left of the red lines represent the fraction of total scattering that does NOT contribute to attenuation for instruments with acceptance angles at the horizontal position of the red line (0.0269, 0.93 and 1.2°) corresponding to instruments whose measurements we analyze here (Table 1).

Different manufacturers have built beam transmissometers having different acceptance angles. The effect of acceptance angle on attenuation has been addressed before (e.g. see [1,8,9]) and several corrections have been suggested [8]. Pegau et al. discuss at length the ramifications of acceptance angle in hydrological optics [9]. For example, the acceptance angle does not have to be very small in studies of ocean color (several degrees should suffice for most applications). However, near forward scattering is important in the case of image propagation through a medium. Measurements with instruments having very small acceptance angle, however, may be affected by scattering by density fluctuations within the water. In such cases, measured beam attenuation represents a time-dependent IOP that is not well correlated to the in-water constituents of interest [9,13-15].

Here we compare particulate beam attenuation data computed from transmission measurements with several commercially available transmissometers deployed together. We are aware of a single study where two vertical profiles of attenuation were measured concurrently with two commercial transmissometers exhibiting, on average 18% difference in reported attenuation [16]. Within a single tidal period, we find that the measured beam attenuations using different transmissometers can differ by less than 10% to as much as 60%. Unfortunately, unless the (time and space-varying) volume scattering function in the near-forward direction is known, there is no way to reconcile these measurements because the transfer function between them is unknown.

The classical theory of light interaction with particles indicates that the acceptance angle acts as a low-pass filter on the particulate size distribution, since for large particles a larger proportion of the scattered light is collected by the detector and is not counted as being attenuated. To illustrate this, we use Mie theory (strictly applicable for homogeneous spheres, but relevant to the attenuation and near forward scattering by randomly oriented non-spherical particles [17]) to compute the proportion of scattering collected by the detector for particles

#104741 - $15.00 USD Received 4 Dec 2008; revised 15 Jan 2009; accepted 16 Jan 2009; published 26 Jan 2009

with three different indices of refraction typical for marine particles such as phytoplankton, bacteria and an inorganic particle near 670nm (n=1.05+i0.005, n=1.05+i0.0001, n=1.15+i0.0001, Fig. 2). Large differences in the contribution of particles larger than 10μm to scattering (and hence to the beam attenuation) are found (Fig. 1) and will result in different beam attenuation measured by instruments with different acceptance angles (Fig. 1). In addition, as particles increase in size towards the geometric optics regime, the effect of composition on scattering (e.g. variation in the real part of n) decreases, because diffraction dominates near-forward scattering (see detailed discussion in ch. 3 of Jonasz and Fournier [17]).

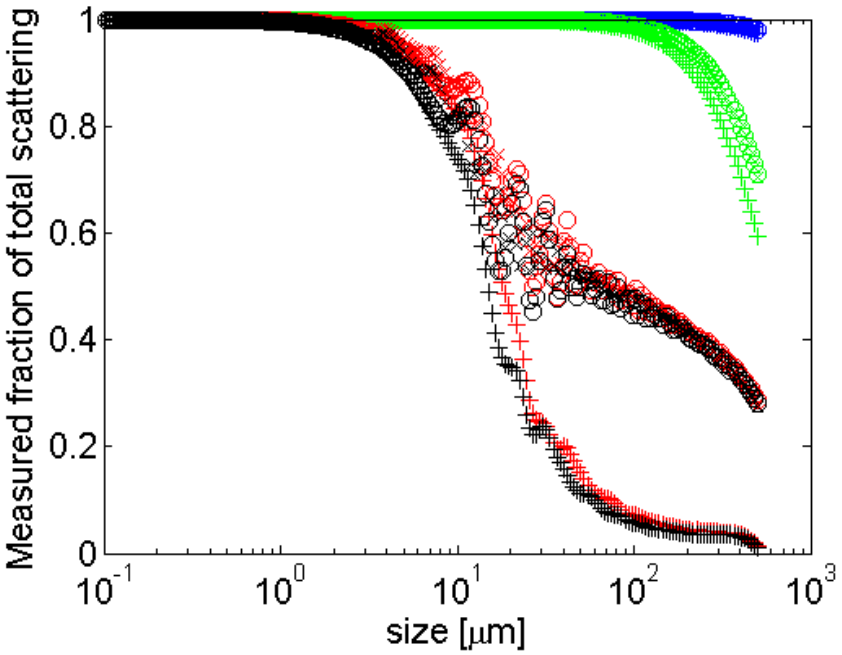

Fig. 2. Ratio of scattering coefficients based on integrating the VSF (β) from π to the acceptance angle to the total scattering coefficient for homogeneous spheres with three different indices of refraction (n=1.05+i0.005 (+), n=1.05+i0.0001 (o), 1.15+i0.0001 (x)) and four different acceptance angles matching those of the instruments we compare in this paper (1.2°-black, 0.93°-red, 0.026°-green, and 0.006°- blue, Table 1) as function of size.

On the other hand, for particles large relative to the measurement wavelength, half of the attenuation is due to absorption (geometric optics regime, e.g. see [7]). The relative role of absorption increases with size to half the total beam attenuation at an e-folding rate equal to 4π times the particle diameter times the imaginary part of the index of refraction divided by the wavelength. For the particles of interest here, absorption will reach a quarter of the total attenuation between about 15μm to 700μm, depending on the imaginary part of the index of refraction (Im(n)=0.005 or 0.0001 respectively). The above discussion implies that for particles increasing in size the effective attenuation cross-section asymptotes the cross-sectional area of the particle (due to absorption), as opposed to theoretical result (relevant to an idealized sensor with zero acceptance angle) of twice the cross-section.

The issue of acceptance angle influence on the measured beam attenuation has important implications on the application of optical transmission data as a proxy of biogeochemical properties (e.g. as surrogates for particulate mass and POC, [16]), as input into sediment transport models, and for visibility modeling (e.g. see [18]). In many of these applications the desired parameter is empirically related to the beam attenuation or it's reciprocal. For

#104741 - $15.00 USD Received 4 Dec 2008; revised 15 Jan 2009; accepted 16 Jan 2009; published 26 Jan 2009

example, many historical relationships have been established with the SeaTech transmissometer (acceptance angle 1.03° [4]), yet proxies are now calculated using beam attenuation measured by other transmissometers, such as the WETLabs C-Star (acceptance angle 1.2°, e.g. see [7,19]), or WETLabs ac-9 (acceptance angle 0.93°, e.g. see [20]). Our results reinforce those of Bishop and Wood [16] and imply that empirical formulations linking the beam transmission to biogeochemical parameters need to be formulated to include the acceptance angle with which they were derived (e.g. they are acceptance angle specific) and that caution should be used when comparing data across instruments.

2. Methods

We used a total of eight commercially available beam transmissometers: (1) a WET Labs 10cm pathlength C-STAR, (2) a WET Labs 25cm pathlength C-STAR, (3) WET Labs ac9 with 10cm pathlength, (4) ac-9 with 25cm pathlength, (5) ac-S with 25cm pathlength, (6) Sequoia Scientific's LISST-100 Type-B, (7) Sequoia Scientific's LISST-100X Type-B and (8) LISST-100X Type-floc (see Table 1 for other pertinent details regarding these instruments). The LISST instruments have a laser light source (highly collimated, monochromatic, and polarized) centered at 670nm, while the WET Labs transmissometers use an unpolarized incandescent lamp collimated using a lens and with a FWHM wavelength range around 676nm of 10nm (ac-9s), 15nm around 650nm for the ac-S or 20nm around 650nm (C-star).

Table 1. Collimated commercial beam transmissometers whose measurements we compare in this study. For the ac meters we only display information for the wavelength used here. For reference the common Sea Tech transmissometer had an acceptance angle of 1.03° [4], a 660nm wavelength and a pathlength of 25cm.

Instrument	Manufacturer	Acceptance Angle (degrees, in-water)	Pathlength	Wavelength (bandwidth)	Beam Diameter
C-STAR-10	WETLabs	1.2	10cm	650 (20)nm	15mm
C-STAR-25	WETLabs	1.2	25cm	650 (20)nm	15mm
AC-9-10	WETLabs	0.93	10cm	676 (10)nm	8mm
AC-9-25	WETLabs	0.93	25cm	676 (10)nm	8mm
AC-S-25	WETLabs	0.93	25cm	650(15)nm	8mm
LISST-100-B	Sequoia Scientific	0.0269°	5cm	670 (0.1)nm	6mm
LISST-100X-B	Sequoia Scientific	0.0269°	5cm	670 (0.1)nm	6mm
LISST-100X-Floc	Sequoia Scientific	0.006°	5cm	670 (0.1)nm	6mm

The instruments were used at a variety of sites and with different configurations and sampling methods. An hourly time series of measurements was conducted to characterize tidal effects on hydrographic and optical properties in the Damariscotta river estuary, Walpole, ME. Sampling was conducted from 4pm on August 4th to 9pm on 5th 2003, near the University of Maine's Darling Marine Center's (DMC) floating dock at a water depth averaging 10m. A 25cm path-length ac-9 and a 10cm path-length C-Star were deployed on the same profiling package from a boat anchored 10m off the DMC's floating dock. A LISST-100-B was deployed on a different package within 10min from the measurements with the other transmissometers. LISST-100-B measurements were taken at 1m depth intervals with the package at rest and then averaged over 1 minute time intervals. C-Star and 25cm path-length ac-9 data were binned to the LISST depth with profiles taken within 10min being considered instantaneous (as the largest cause for variability was due to the tides).

#104741 - $15.00 USD Received 4 Dec 2008; revised 15 Jan 2009; accepted 16 Jan 2009; published 26 Jan 2009

A second coastal study utilized a large instrumented tripod deployed for several weeks during the fall of 2005 near the Woods Hole Oceanographic Institution, Martha's Vineyard Coastal Observatory (MVCO) as part of the ONR funded Optics, Acoustics and Stress In Situ (OASIS) project. In this case, the 10cm path-length ac-9, LISST-100X-B and LISST-100X-Floc transmissometers were deployed on the same tripod 1.2m above the bottom at a site 12m deep off the south coast of Martha's Vineyard. Maximum distance between instruments was 1m and all data were binned to 1minute bins. Beam attenuation by the ac-9 at 676nm was computed from the difference between the measured beam attenuation and the beam attenuation measured when the water was diverted through a 0.2μm filter. The volume scattering function (e.g. Fig. 1) was merged from the two LISST instruments and based on bead calibrations as described in Slade and Boss [21].

In 2007, a 25cm ac-S and a 25cm C-star were in-line to measure optical properties on a flow-through of seawater sampled from about 3m depth in a cross-equatorial transect as part of a NASA funded Equatorial Box project. Beam attenuation of particles at 650nm was computed from the difference between the measured beam attenuation and the beam attenuation measured when the water was diverted through a 0.2μm filter (see Dall'Olmo et al. for complete details regarding the setup [22]).

Finally, we performed an aggregation experiment in the laboratory in order to examine how aggregation affects optical properties as a function of increasing aggregate size [23]. Two beam transmissometers (a LISST-100 Type B, acceptance angle 0.0269° and a 10cm path-length ac-9, acceptance angle 0.93°) were arranged side by side in a large sink with their sampling volumes open to the environment near the bottom. Both instruments were positioned to sample at the same depth of 16cm above the bottom of the sink. The sink was then filled with particle-free reverse-osmosis water, which provided blank values for all instruments. A slurry of bentonite clay was disaggregated by vigorous stirring for ~30 minutes, added into the sink, and then mixed into the water (4g dry weight in 120L of water). Salt was then mixed into the sink to initiate aggregation.

In the field deployments with the ac-9, ac-S, and C-star measurements, we subtracted measurements taken using a 0.2μm filter on the instrument intake yielding calibration-independent particulate beam attenuation. The purpose of this procedure was not to remove CDOM absorption (which is low at wavelengths greater than 650nm), but rather to remove possible instrumental drift [24] and biofouling. The LISST instruments were deployed such that their optical path was open to the ambient environment in the vertical direction (particles could settle vertically through the optical path yet sideways motion was hindered by the sensor's head). Throughout this paper the reported beam attenuation (denoted by c or c_{pg}) does not include the contribution of pure water. The contribution of dissolved materials to attenuation in the reported wavelength (between 650-676nm) where we sampled is assumed negligible. When we explicitly removed the dissolved fraction from the measurements of attenuation (e.g. using a calibration independent technique) the attenuation is that of particles only (denoted by c_p).

3. Results

3.1 Darling Marine Center (DMC)

Tidal dynamics dominated the beam attenuation at the DMC (Fig. 3) and the three measurements of beam attenuation were very different. Maximum in beam attenuation correlate with the maximum in the ebb tide (not shown). The smaller the acceptance angle of a given instrument (Table 1), the higher the beam attenuation measured. The ratios of beam attenuation for the different instruments varied with the tide. The C-Star to LISST-B ratio was on average 0.7 and varied between 0.55 and 0.9 (variance reported here and below is the 5^{th} to 95^{th} percentile for all measurements of the ratio). The ac-9 to LISST-B ratio was 0.79 and varied from 0.60 to 1.04. Finally, the C-Star to ac-9 ratio averaged 0.90 and varied from 0.55

#104741 - $15.00 USD Received 4 Dec 2008; revised 15 Jan 2009; accepted 16 Jan 2009; published 26 Jan 2009

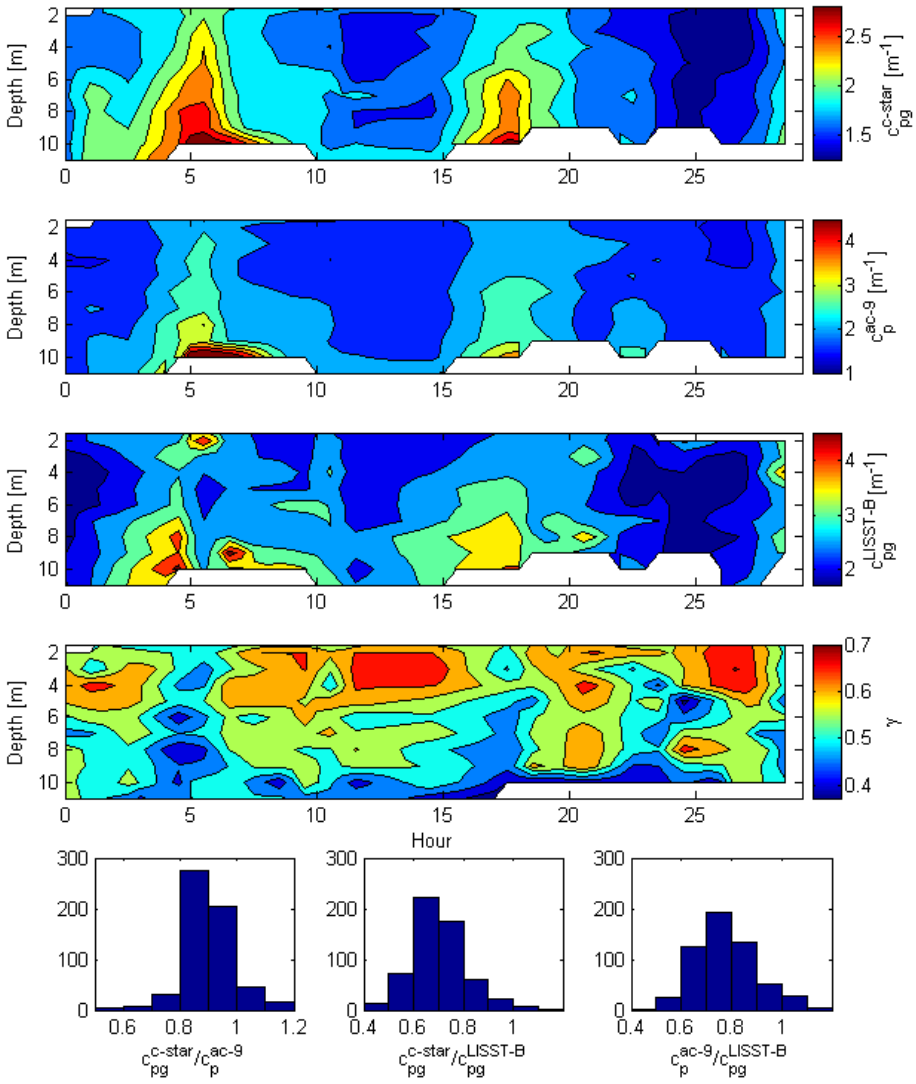

Fig. 3. Measurements taken 10m off the Darling Marine Center pier. Top panels: time series of the beam attenuation (660nm) measured with a 10cm pathlength c-star (top), measured with a 25cm ac-9 at 676nm (2nd from top) and measured with a 670nm LISST-B (3rd from top). Time series of the spectral slope of the beam attenuation coefficient (γ) based on the spectral measurements of the ac-9. Note: The color scale varies between the panels and that the LISST was not deployed at the same time or with the same package as the two other instruments (see text). Bottom panel: histograms of the frequency of occurrence of the ratios among the measured beam attenuations.

to 1.06 (Fig. 3). The spatial and temporal variability in the C-Star/ac-9 ratio correlates positively (though weakly) with the spectral slope of the particulate beam attenuation (R=0.4). The spectral slope of the particulate beam attenuation (γ) is a size parameter that correlates negatively with mean particle size (e.g. see [25]). The larger the mean particle size (consistent with smaller γ), the smaller the ratio of C-star/ac-9 (hence a positive correlation),

#104741 - $15.00 USD Received 4 Dec 2008; revised 15 Jan 2009; accepted 16 Jan 2009; published 26 Jan 2009

consistent with the expectation that the scattering portion of attenuation will be most different among transmissometer with varied acceptance angle when large particles are present (e.g. Fig. 2 and the Introduction). Thus, both the magnitude of the beam attenuation ratio and its variability are consistent with effects of particle size and acceptance angle (e.g. Fig. 1 & 2) on measured attenuation. Note, however, that the ac-9/LISST-B and C-star/LISST-B ratios did not correlate with γ (R~0).

3.2 Martha's Vineyard Coastal Observatory (MVCO)

Time series of beam attenuation for the three transmissometers of differing acceptance angles deployed at MVCO all exhibited similar first-order temporal trends, showing an increase in attenuation as stratification diminishes that was modulated by the tidal cycle and periodic storms (Fig. 4). However, the absolute values of the three estimates of the beam attenuation were significantly different, with magnitudes varying as expected based on differences in acceptance angle. On average, the ratio of ac-9 to LISST-B was 0.64 and varied from 0.46-0.84. The ac-9 to LISST-Floc ratio averaged 0.56 and varied from 0.4 to 0.73. The highest ratios occurred during times of maximum particle concentrations (Fig. 4). The LISST-B to LISST-Floc ratio varied less, from 0.77 to 1 with an average of 0.88 (Fig. 4). The beam attenuation spectral slope exhibited a strong and inverse correlation with the ratios of beam attenuation (R=-0.65, for $c_{p,ac9}/c_{p,LISST\text{-}B}$ ratio). This inverse correlation is surprising because it means that the different measures of beam attenuation are in better agreement when the mean particle size is large rather than small. These observations are counter-intuitive as we expect the scattering portion of attenuation to be most different among transmissometer with varied acceptance angle when large particles are present (e.g. Fig. 2).

3.3 Cross-equatorial transect

In the open ocean, the variability in beam attenuation over a 1500km transect was smaller than that observed over tidal cycles in the coastal environment (contrast Fig. 4 and Fig. 5). Despite this reduced dynamic range, we did find that beam attenuation measured by the ac-S and a C-star were very well correlated (R=0.99), with nearly a constant ratio between instruments (mean ratio of 0.83, Fig. 5). Modulations in this ratio had an even smaller dynamic range than the magnitude of attenuation and was correlated positively with the slope of the particulate beam attenuation, a size parameter (R=0.5, Fig. 5). On average, when the mean particulate size increased (γ is reduced), the ratio between the C-Star beam attenuation to that of the ac-s was reduced, consistent with expectations for different acceptance angles and scattering effects from variability in particle population sizes. The average relative difference (17%) here between the transmissometers, is consistent with that reported for transmissometers of the same acceptance angle by Bishop and Wood (18%, [16]) in the North West Pacific Ocean (note typo in [16] where the C-star acceptance angle is stated as1.5°).

#104741 - $15.00 USD Received 4 Dec 2008; revised 15 Jan 2009; accepted 16 Jan 2009; published 26 Jan 2009

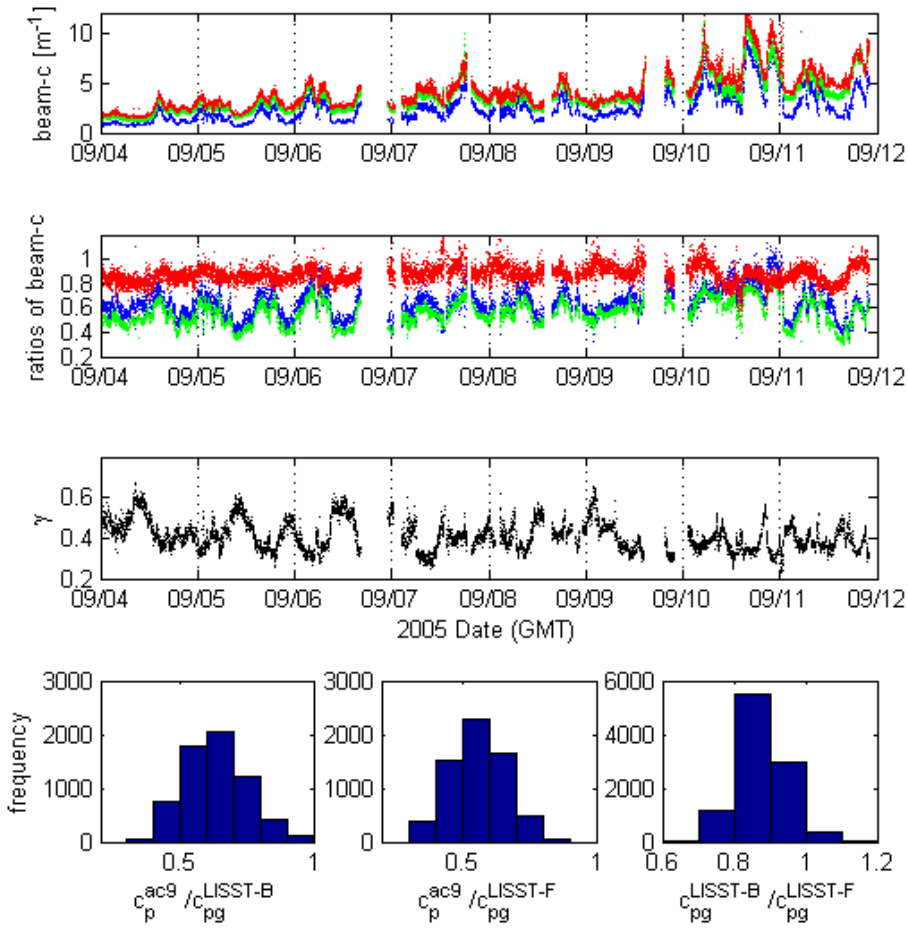

Fig. 4. Top panel: time series of 1-min averages of the beam attenuation measured with a 10cm pathlength ac-9 (blue), LISST-100X-B (green) and LISST-100X-Floc (red). Second panel: time series of the ratios of 1-min averages $c_{p,ac\text{-}9}/c_{pg,LISST\text{-}B}$ (blue), $c_{p,ac\text{-}9}/ c_{pg,LISST\text{-}FLOC}$ (green), and $c_{pg,LISST\text{-}B}/ c_{pg,LISST\text{-}FLOC}$ (red). Third panel: time series of the spectral slope of the particulate beam attenuation (γ). Bottom panel: histograms of the frequency of occurrence of the ratios depicted in the second panel.

#104741 - $15.00 USD Received 4 Dec 2008; revised 15 Jan 2009; accepted 16 Jan 2009; published 26 Jan 2009

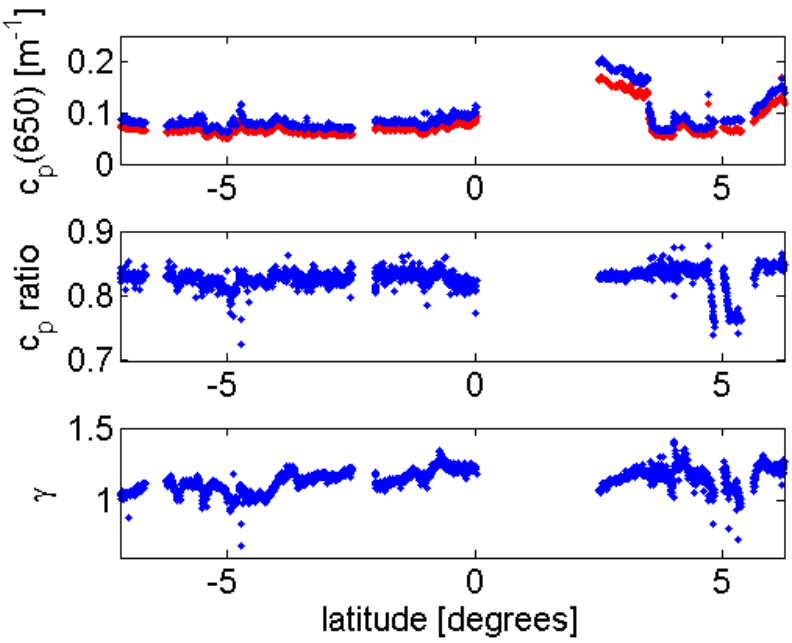

Fig. 5. Top panel: spatial distribution of 1-min averages of the beam attenuation measured with a 25cm path-length ac-s (red) and a C-Star (blue) measured across equatorial Pacific at 140°W at 650nm (N=2397). Middle panel: spatial distribution of the ratios of 1-min averages $c_{C\text{-}Star}$/ $c_{ac\text{-}s}$. Bottom panel: spatial distribution of the spectral slope of the particulate beam attenuation, γ, a size-related parameter, where smaller γ implies larger mean particle size [24].

3.4 Aggregation experiment

During the laboratory experiment, we observed a change in the mean particle diameter from 7 to about 70μm (as derived from LISST measurements) as aggregates formed and settled (Fig. 6). The presence and size of aggregates was confirmed qualitatively with microphotography on discrete samples. Simultaneous with the increase in size, we recorded an increase in the LISST-B to ac-9 beam attenuation ratio. This change is consistent with size-acceptance-angle effects on the relative contribution of scattering to beam attenuation.

#104741 - $15.00 USD Received 4 Dec 2008; revised 15 Jan 2009; accepted 16 Jan 2009; published 26 Jan 2009

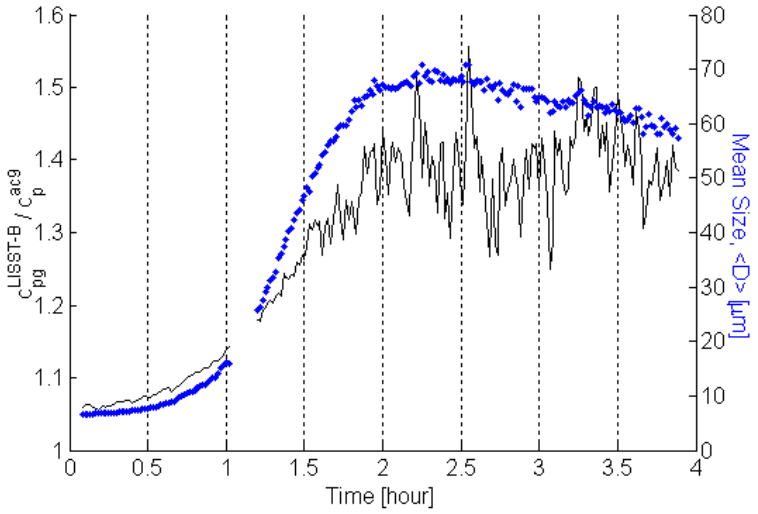

Fig. 6. Aggregate size as function of time (blue line) and the corresponding ratio of the beam attenuation measured by the LISST-B at 670nm to that of the ac-9 at 676nm as function of time as measured during a laboratory clay aggregation experiment. Oscillations in the ratio are due to decrease of signal to noise ratio as the water clarifies of settling particles ($c_{pg,LISST-B}$ decreased from $12m^{-1}$ to $3m^{-1}$ during the experiment).

4. Discussion

We observed large differences in measured beam attenuation using eight different commercial transmissometers. The relative magnitudes of the measured beam attenuation most often show that the larger the acceptance angle of an instrument (Table 1), the smaller the measured beam attenuation. In rare occasions we find beam attenuation ratios bigger than one (DMC and MVCO) between a transmissometer with a large acceptance angle to one that has a smaller acceptance angle. This is most likely due to measurement errors, spatial variability and/or deployment methodology (e.g., comparing pumped ac-9 with unpumped LISST). In addition, we commonly found that the larger the mean particle size, the smaller the ratio of beam attenuation measured with a wide acceptance angle to that for a narrow acceptance angle, which is consistent with the decrease in proportion of scattering that is inferred when measure transmission with increasing acceptance angle (Fig. 2). This correlation with size, however, is rather weak and, for the MVCO observations, actually varied in the opposite direction as expected based on size-acceptance-angle-scattering considerations alone. The ratio of ac-9/LISST-B was also uncorrelated with the size parameter in the DMC dataset.

To assist in understanding the MVCO results, we use independent information on volume scattering function provided by the LISST instrument and calibrated following Slade and Boss [21]. Volume scattering functions were merged from the two LISSTs (for the MVCO dataset) and then integrated from the acceptance angle of the ac-9 to that of the LISST-B. This scattering was then added back to the ac-9 beam attenuation ($c_{p,\,ac9}$), assuming that the spectral difference between instruments has a negligible effect:

$$c_{p,ac9\,corrected} = c_{p,ac9} + 2\pi \int_{\theta_{LISST-B}}^{\theta_{ac-9}} \beta \sin\theta \, d\theta. \qquad (5)$$

#104741 - $15.00 USD Received 4 Dec 2008; revised 15 Jan 2009; accepted 16 Jan 2009; published 26 Jan 2009

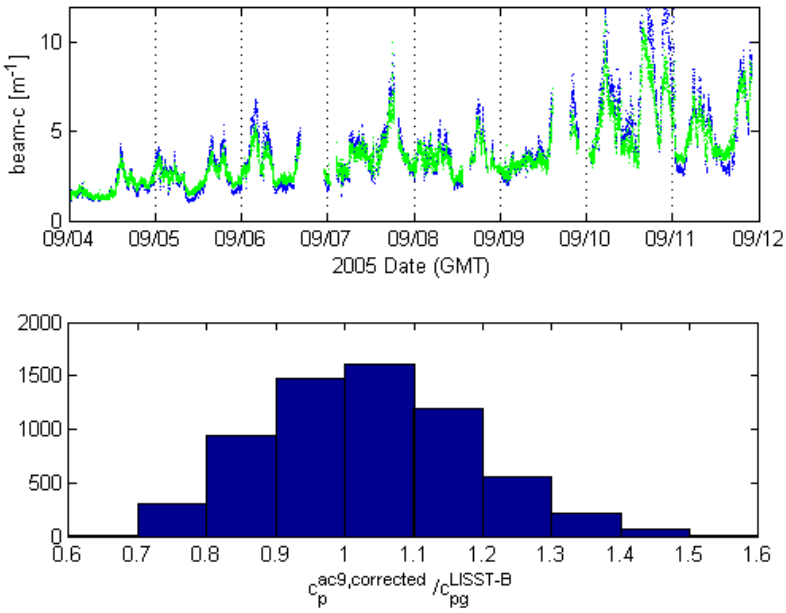

Fig. 7. Top panel: time series of 1-min averages of the beam attenuation measured with a 10cm pathlength ac-9 corrected for acceptance angle difference as in Eq. (5) (blue), LISST-B (green). Bottom panel: histograms of the frequency of occurrence of the ratio of the two time series depicted in the top panel.

The above correction does, on average, bring the ac9 beam attenuation into agreement with that of the LISST-B (The average c_p ratio changes from 0.64 to 1.03, compare Figs. 4 and 7). Differences in absolute value that are not reconciled using this procedure remain, however, but are usually smaller than 20%. In particular, the corrected ac9 beam attenuation has a wider range than that of the LISST-B (Fig. 7).

Differences remaining between corrected-ac-9 beam attenuation and that of the LISST are likely due to important differences in the geometry of the instruments and the method of deployment. The instruments have a different pathlength (Table 1), with the ac-9 being more susceptible to multiple scattering when attenuation is large. This is likely to result in larger estimated beam attenuation by the ac-9, due to increases in the average photon pathlength and particularly from multiple near-forward scattering of light away from the detector [26]. In addition, water is drawn through the ac9 flow tube using a pump. Such pumping may break large particle aggregates and change their optical properties. On the other hand, the LISST's head geometry may also interfere with the measured particles, as it is open to falling particles but has two supporting walls that obstruct sideways advection of particles and flow. Minor bio-fouling of the LISST may also contribute to differences between instruments towards the end of the time series. The ac-9 measurements, in contrast, are computed from differences of separate total and dissolved measurements and are thus immune to minor instrument biofouling and drift. Despite these differences, we find VSF variability measured by the LISST sufficient for explaining a bulk of the differences between attenuation values, suggesting that differences in path-length and deployment methodologies are constrained to within about 20% (Fig. 7).

To better understand the nature of the difference between the measurements at MVCO, we analyzed an additional size parameter, the median particle size based on the LISST inversion (e.g. see [27]). This parameter and the spectral slope of the beam attenuation both indicate that larger particles are present at larger percentage when the ratio of ac-9 corrected c_p to $c_{pg,LISST-B}$

#104741 - $15.00 USD Received 4 Dec 2008; revised 15 Jan 2009; accepted 16 Jan 2009; published 26 Jan 2009

is largest (Fig. 8). This covariation with size is opposite of expectations based on scattering consideration and Mie theory and requires explanation. First, it may suggest a causal relationship, i.e. that samples with large mean particle sizes are enriched with aggregates. These aggregates break within the ac-9 resulting in more scattered light collected by the ac-9 receiver and hence to better agreement. In a separate experiment we did, indeed, find that breaking aggregates increases the beam attenuation (not shown). An additional possibility is that absorption provided a higher portion of total attenuation by large particles, thus countering the tendency of scattering. Alternatively, a non-causal relationship may be in effect, whereby multiple scattering enhances c_p measured by the ac-9 relative to the LISST-B at high concentration and that the relationship with size is due to the known general co-variation of size and concentration in the bottom boundary layer due to the faster settling rate of large particles [25].

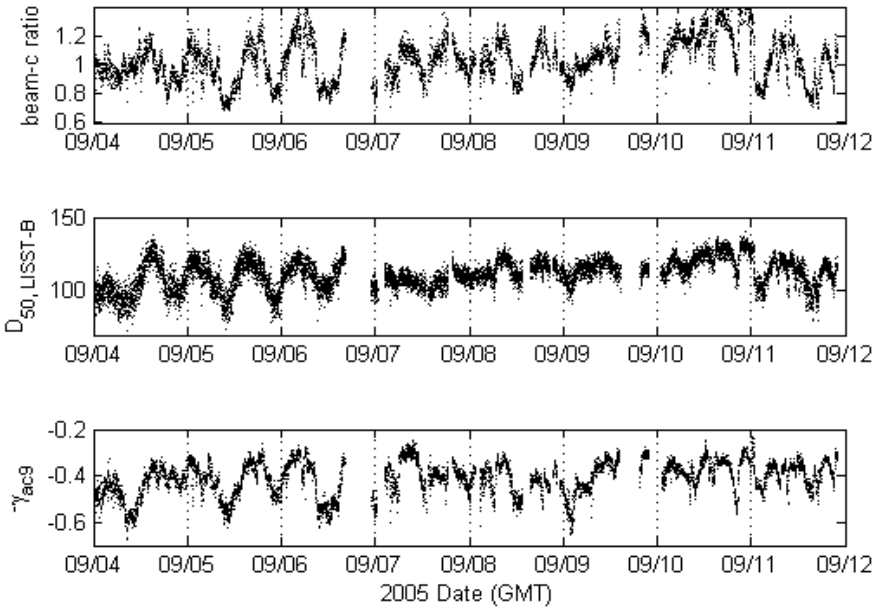

Fig. 8. Top panel: time series of the ratio of 1-min averages of the beam attenuation measured with a 10cm pathlength ac-9 corrected for acceptance angle difference as in Eq. (5). Middle panel: Median diameter based on the LISST inversion of VSF to particulate size distribution. Bottom panel: slope of the spectral particulate beam attenuation of the ac-9.

The contribution of large particles to the beam attenuation depends also on concentration. When particle concentration in the illuminated sample falls below about 400 within the sampled volume, they are not well approximated as a continuum and will appear as spikes [28,29]. Some transmissometers include an R/C circuitry that filters out isolated spikes, which would effectively filter out large particles when they are present in low concentrations. Similarly, median averaging in space or time filters out the contribution of poorly sampled particles to the processed signal. Thus, processing, sample size and engineering issues can all contribute to variations in reported beam attenuation between sensors, regardless of acceptance angle.

Scattering by turbulence in the sampled water (due to fluctuation in the index of refraction of water, e.g. see [13,14]) may represent another potential contributor to observed differences in beam attenuation measured by instruments with different acceptance angles. Such scattering has been documented for LISST instruments when profiled in waters with high

#104741 - $15.00 USD Received 4 Dec 2008; revised 15 Jan 2009; accepted 16 Jan 2009; published 26 Jan 2009

density gradients [15]. However, we do not believe that turbulence was an important contributor to the measurements presented here because measurements for MVCO were conducted in a bottom boundary layer that was highly mixed in density and had temperature dissipation rates on the order of $\chi \sim 10^{-7} °C^2/s$ [30]. According to Bogucki et al. [14], temperature dissipation rates on the order of $10^{-5} °C^2/s$ and larger are needed for turbulence to make a significant contribution to scattering within the acceptance angle of the LISST-B. In addition, the size parameter derived by the ac-9 (a pumped instrument that does not experience the environmental turbulence) co-varied with that of the LISST-B (which is open to environmental turbulence, Fig. 7), suggesting that turbulence was not an important factor at MVCO.

Diver visibility has been found to be inversely proportional to beam attenuation (e.g. see [18]), but sensitivity of this relationship to the acceptance angle has not been studied. We anticipate such a visibility index will be sensitive to the acceptance angle and that the appropriate one to use is likely to be associated with the spatial angle occupied by an object within the field of view of the diver. Future modeling and environmental testing is needed to understand that sensitivity.

Our results may also have implications on the interpretation of diel cycles in c_p that have been observed throughout the world's ocean (e.g. see [31,32,33,34,35]). These cycles are associated with changes in beam attenuation as large as 30-50% between day and night ([33,34]) and have been interpreted as changes in concentration and/or sizes of phytoplankton cells and/or changes in their index of refraction (e.g. see [35]). The effect of acceptance angle on this cycle (as cell size changed) has not been discussed to date and merits attention, as its effect can be significant. For example, the doubling in volume of a 12μm organic cell (n=1.05+i0.0001) will cause a 50% reduction in volume-normalized (hence mass- or POC-normalized) c_p measured by a transmissometer with a 1.2° acceptance angle at a weakly absorbing wavelength (Fig. 2). On the other hand, the acceptance angle effect is likely to be significantly smaller in the oligotrophic areas of the ocean that where pico-plankton are abundant [e.g. 33]. We recommend that this measurement artifact be investigated (e.g. using sensors with different acceptance angle) to insure that the interpretation of these cycles is consistent with ecosystem process.

5. Summary

We observed large and time-varying differences in beam transmission measured by eight different commercial transmissometers. In all cases, the magnitude of the beam attenuation decreased with increasing acceptance angle, as expected. Unfortunately, variability in the ratio over time and space precludes the possibility of having a simple fix (e.g. a constant to multiply with that will take care of the difference), particularly for measurements in coastal locations and bottom boundary layers where the particulate size distribution and the particulate composition are often highly variable. As demonstrated here, if the time-varying volume scattering function is available the different estimates of the beam attenuation can be, to a large degree, reconciled (Fig. 7).

An important implication of our results is that they demonstrate that the acceptance angle needs to be reported when using beam attenuation as a surrogate of a biogeochemical variable (see also [16]). In environments with relatively stable size distribution, a constant conversion factor may relate measurements with one acceptance angle to another (e.g. Fig. 5).

Our observations suggest that reevaluation may be necessary in accepted relationships between beam attenuation and biogeochemical parameters, beam attenuation and visibility, and in the interpretation of diel cycles in the beam attenuation and ecosystem dynamics.

Practically, however, we find that the ratios of beam attenuation of different instruments do not always follow an evolution that is expected from size dynamics alone. We conclude that more work needs to be done with the oldest (in terms of availability of commercial in-situ instruments) and simplest (so we thought…) optical property, the beam attenuation.

#104741 - $15.00 USD Received 4 Dec 2008; revised 15 Jan 2009; accepted 16 Jan 2009; published 26 Jan 2009

Acknowledgments

This work has been funded by the optics and biology program of the Office of Naval Research (N00014-04-1-0235) and the National Aeronautics and Space Administration ocean biology and biogeochemistry program (NNG05GD18G) and has benefited from discussions with Paul Hill, John Trowbridge, Tim Milligan, Yogi Agrawal, Allan Weidemann, Ron Zaneveld and Mike Twardowski. Comments by Hubert Loisel and an anonymous reviewer have improved the manuscript significantly. The data were collected and partially processed with the help of Trish Bergmann and Jim Loftin.

#104741 - $15.00 USD Received 4 Dec 2008; revised 15 Jan 2009; accepted 16 Jan 2009; published 26 Jan 2009